



DOI: doi.org/10.21009/SPEKTRA.072.03

IMPLEMENTATION OF TRS-398 PROTOCOL IN ROUTINE CALIBRATION OF LINAC BY DETERMINATION OF SLAB PHANTOM ON WATER PHANTOM CORRECTION FACTOR

Azizallah Fauzi¹, Fitrotun Aliyah^{1,*}, Darmawati²

¹*Department of Nuclear Engineering and Engineering Physics, Faculty of Engineering, Universitas Gadjah Mada, Yogyakarta, Indonesia*

²*Radiotherapy Installation, RSUP Dr. Sardjito, Yogyakarta, Indonesia*

*Corresponding Author Email: fitrotun.aliyah@ugm.ac.id

Received: 1 August 2022
Revised: 21 September 2022
Accepted: 22 September 2022
Online: 28 September 2022
Published: 30 September 2022

SPEKTRA: Jurnal Fisika dan Aplikasinya
p-ISSN: 2541-3384
e-ISSN: 2541-3392



ABSTRACT

The water phantom is used for LINAC calibration to measure absorbed dose radiation. Practically, it requires a long preparation time and is considered less efficient. To increase efficiency, the medical physics team in a hospital uses slab phantom as the calibration tool. Consequently, the correction factor is crucial to define the equivalence of the absorbed doses resulted from slab phantom. The absorbed dose measurement was performed according to the IAEA TRS-398 dosimetry protocol with a cylindrical ionization chamber detector for 6 MV photon beam and electron beams from Elekta Synergy Platform 154029 LINAC with 6 MeV, 8 MeV, 10 MeV, and 12 MeV energy variations. The field size for slab and water phantom is 30 cm x 30 cm x 30 cm. Based on the TRS-398 protocol, the correction factor of the slab phantom calculated based on absolute dosimetry for 6 MV photons beam, the electron beam of 6 MeV, 8 MeV, 10 MeV, and 12 MeV are 1.0018; 0.9995; 0.9979; 1.0041 and 1.0068, respectively. As a result, the absorbed dose radiation measured by the calibrated slab phantom using the resulted correction factor has an equivalent amount to the water phantom.

Keywords: dosimetry, slab phantom, water phantom, IAEA TRS-398, LINAC

INTRODUCTION

Radiotherapy, as the most widely used treatment to kill cancer cells, use a high ionization radiation [1]. Radiotherapy can be categorized as a fairly complex method because it involves many staff groups and consists of multiple steps in preparing and delivering radiation doses during treatment, aiming to improve the accuracy of radiation dose delivery in radiotherapy [2,3].

The principle of radiotherapy is optimizing the administration of radiation doses to the targeted volume (cancer cells) and minimizing the effects of radiation on healthy tissue around the target. Based on the placement of the source of radiation, radiotherapy can be classified to external radiation and internal radiation. External radiation therapy uses a beam externally directed to treat deep cancer cells within the body. In contrast, internal radiation is applied by inserting a radiation source directly into tumor cells or adjacent body parts using brachytherapy or radiopharmaceuticals [4].

A Linear Accelerator (LINAC) utilizes high-frequency electromagnetic waves to speed up electrons for high energies around 4-25 MeV over a linear accelerator waveguide [5,6]. In its application, the output of the LINAC is easily affected by tool setting and environmental conditions. In contrast, the stability of the beam of radiation output of the LINAC greatly influences the dose distribution received by the patient. Therefore, the LINAC requires a routine calibration to control the accuracy of the patient's received dose, which included in the quality control procedures in the quality management system [7,8]. Various dosimetry methods have been developed for calibration with various specified reference conditions both of absolute dosimetry and relative dosimetry, for instance ionometric dosimetry, gel dosimetry, film dosimetry, luminescence dosimetry, and others [9,10,11].

Nevertheless, among these methods, dosimetry of ionometric is still take into account the most appropriate method for calibrating doses in photon radiotherapy because the response given by the ion chamber is fast and active and has high precision for quantification of absorbed dose. As a guide to dose measurement in ionometric dosimetry, two standard dosimetry protocols have been developed are IAEA Technical Report Series No.398 (TRS-398) and American Association of Physicists in Medicine Task Group No.51 (AAPM TG-51) [12-14]. However, TRS-398 protocol is the most commonly adopted and applied radiation dosimetry protocol worldwide [11,15].

Almost all radiotherapy units in Indonesian hospitals use the IAEA TRS-398 dosimetry protocol as their dosimetry guidelines. This Code of Practice (TRS-398) as the new international code to define the water absorbed dose in external beam radiotherapy which uses a dosimeter or an ionization chamber with calibration factor of absorbed dose to water ($N_{D,w,Q0}$), is appropriate in entirely facilities and hospitals serving radiotherapy treatment for cancer patients. Although these institutions' characteristics are probably generally altered, this TRS-398 protocol will assist as an advantageous standard to the medical physics and radiotherapy community and help accomplish equality and steadiness in radiation dose delivery to patients globally. This protocol offers a methodology to determine the absorbed

dose of water from photon beams, electron beams, heavy ion beams, and proton beams in external radiation therapy with an energy range of low, medium, and high energy [16].

LINAC dosimetry measures absorbed radiation dose to a phantom replacement for human tissue. LINAC's dosimetry is consist of two measurements, namely absolute dosimetry and relative dosimetry. In absolute dosimetry, the results obtained are the values of absorbed doses of radiation in gray units (Gy). In contrast, relative dosimetry produces a percentage of doses at various depths and positions. Following the TRS-398, the technical standard for absolute dosimetry measurements in the calibration process of the LINAC is using a water phantom. Meanwhile, this quantity is closely related to the radiation biological effects [13].

Using water phantom in the calibration process of LINAC needs long preparation time [2,13]. The less efficiency of preparation using water phantom will impact the number of daily treated-patients in the hospital. Meanwhile, to shorten the preparation time, the hospital uses slab phantom to substitute the water phantom on daily LINAC calibration. Slab phantom have been widely applied in several foreign institutions, such as Iran using PMMA plastic slab phantom [13], India using tissue equivalent slab phantom with lithium tetraborate [3], Canada using polystyrene slab phantom [17], Turkey with slab head phantom [18], and South Africa with Nylon-12 water equivalent solid phantom [2]. This research aims to determine the correction factor of slab phantom to water phantom for accuracy of absorbed dose measurement in LINAC calibration.

METHOD

Dose Measurement

The measurements were conducted in the Radiotherapy installation of Dr. SARDJITO Hospital, Yogyakarta, Indonesia. The material used in this work are: 1) Linear Accelerator LINAC Elekta Synergy Platform 154029; 2) Farmer detector PTW Freiburg with Chamber TM 30013 type for PDD measurement [7,19]; 3) electrometer; 4) water phantom; 5) slab phantom with the material specification is water equivalent white polystyrene "RW3" for high energy photon and electron energy, with dimension of 30 cm x 30 cm x 30 cm and 1.045 g/cm³ mass-density; 6) barometer; 7) thermometer and 8) electron applicator with 10 cm x 10 cm dimension.

Dosimetry measurements were conducted on the source to a surface distance (SSD) 100 cm with a field area of 10 cm x 10 cm on the phantom surface [7,11,12,19]. The radiation fields used are 6 MV energy photons and electron accelerator with energy 6, 8, 10 and 12 MeV. The applicator only used for radiation of electrons, while radiation for the photon is not used.

To determine the correction factor of slab phantom to water phantom for LINAC Elekta Synergy Platform 154029, the absorbed dose both of water phantom and slab phantom should be measured. The measurement is one of the steps in the LINAC calibration process using IAEA TRS-398. FIGURE 1 shows a schematic of the device used for the measurements, while FIGURE 2 shows the measurement procedure based on IAEA TRS-398.

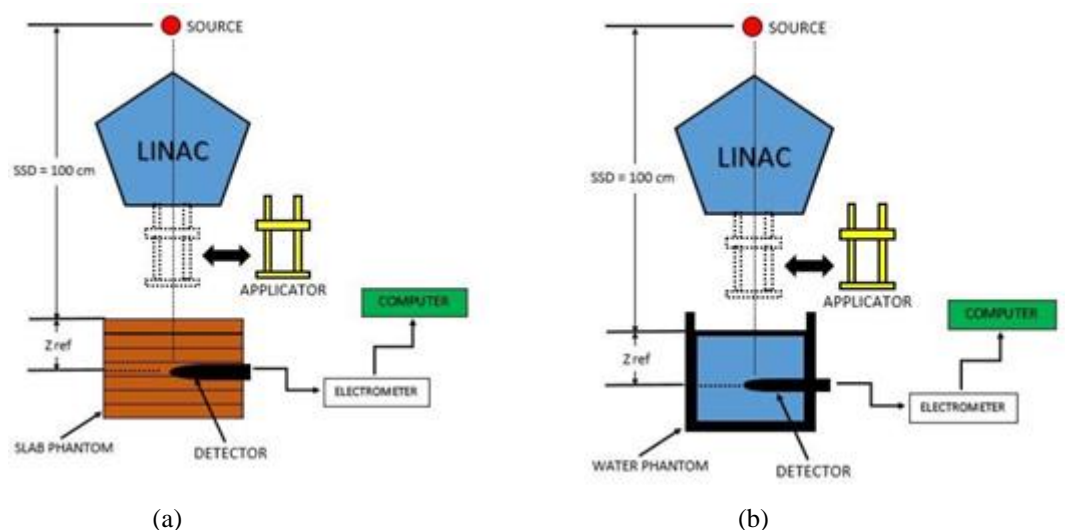


FIGURE 1. Schematic illustration of the phantom to measure the absorbed dose of radiation: (a) slab phantom, (b) water phantom [20].

Relative Dosimetry

The initial measurement was carried out to obtain the radiation beam quality value and the percent depth dose (PDD). The radiation beam quality shows the ability of radiation to penetrate the material that the quality of the beam for a different type and radiation energy. The radiation beam quality values of photon dosimetry ($E = 1-50$ MV) which generated by electrons are $TPR_{20,10}$ (tissue-phantom ratio) while the beam quality in electron dosimetry ($E = 3-50$ MV) is R_{50} . The $TPR_{20,10}$ is the photon dosage ratio at a depth of 20 cm and 10 cm to water phantom, while R_{50} is the depth of phantom where the absorbed dose achieved 50% of the maximum dose. $TPR_{20,10}$ is attained from the measured dose ratio, it does not involve a displacement correction factor at both depths when using a cylindrical chamber. Moreover, $TPR_{20,10}$ in most clinical settings is unaffected by minor errors when positioning the detector at each depth, since setting in both positions will produce the same effect [12]. $TPR_{20,10}$ can also be calculated from fitting to the PDD data at 10 cm depth (PDD_{10}) measured at an 100 cm SSD and a 10 cm x 10 cm field size, see EQUATION (1) [12,21]. Another empirical relationship is also used for calculating $TPR_{20,10}$ using $PDD_{20,10}$ as shown in EQUATION (2)[8,22]. $PDD_{20,10}$ is the PDD ratio at depth of 20 cm to 10 cm.

$$TPR_{20,10} = -0.7898 + 0.0329(PDD_{10}) - 0.000166(PDD_{10})^2 \quad (1)$$

$$TPR_{20,10} = 1.2661(PDD_{20,10}) - 0.0595 \quad (2)$$

The PDD means the percentage of LINAC's radiation output at a certain depth which illustrates the absorbed dose distribution within a patient. PDD is affected by field size, beam energy, and depth for 100 cm SSD. From the results of this relative dosimetry, the reference depth value (Z_{ref}) could be determined as the detector placement position of the phantom. The Z_{ref} value for photon dosimetry stated in EQUATION (3) and (4), and for electron dosimetry stated in EQUATION (5).

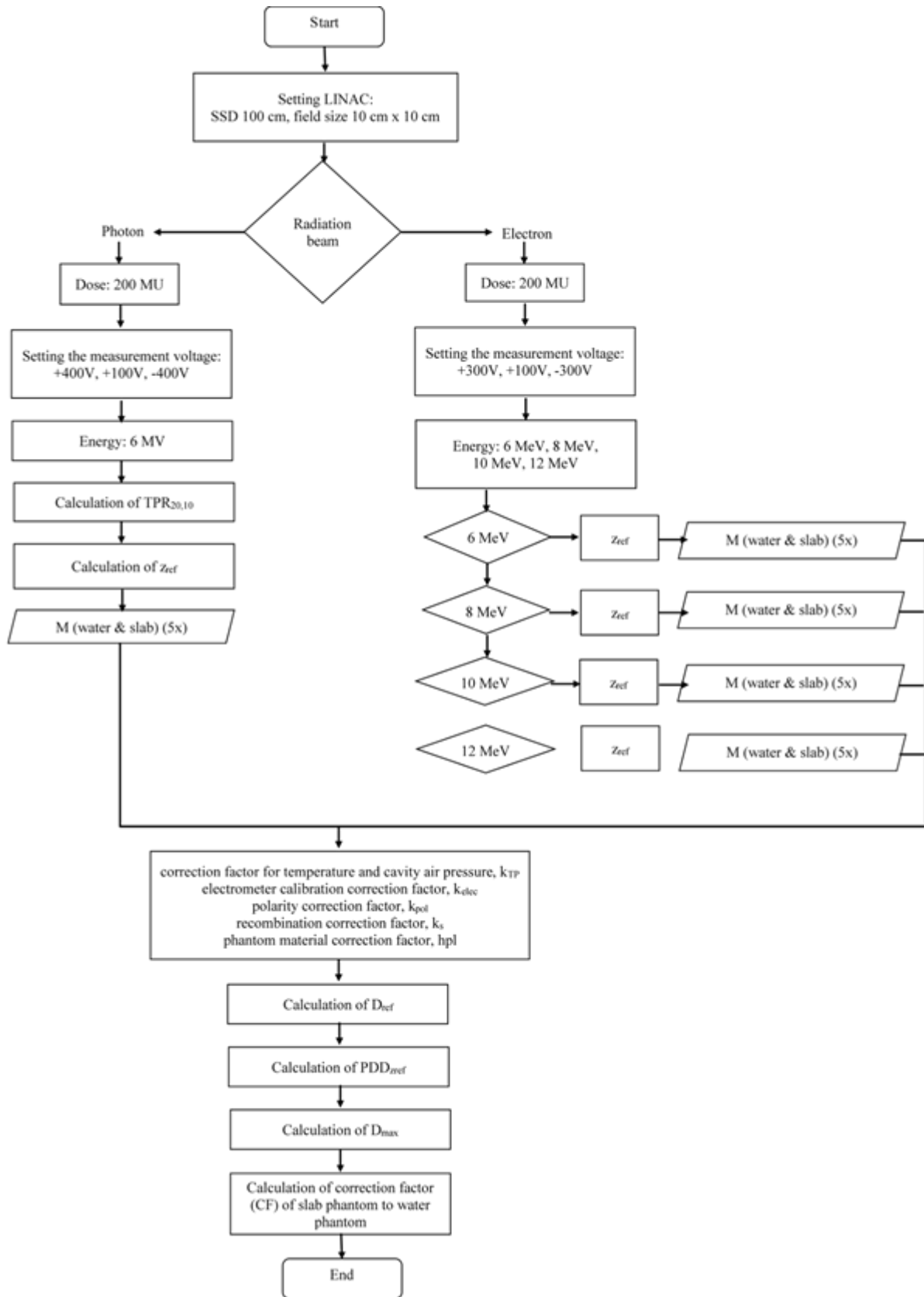


FIGURE 2. The flowchart of measurement process based on IAEA TRS-398 [20]

$$z_{ref-photon} = 10 \text{ g/cm}^2 \text{ or } 5 \text{ g/cm}^2, TPR_{20,10} < 0.7 \quad (3)$$

$$z_{ref-photon} = 10 \text{ g/cm}^2, TPR_{20,10} \geq 0.7 \quad (4)$$

$$z_{ref-electron} = 0.6 R_{50} - 0.1 \text{ g/cm}^2 \quad (5)$$

Absolute Dosimetry

Subsequent measurements were made to obtain the radiation absorbance dose values in the water phantom and slab phantom. According to TRS-398 protocol recommendations [12], absolute dosimetry on high energy photon beams and electrons can be applied according to the following EQUATION (6):

$$D_{w,Q} = M_Q N_{DwQ_0} k_{Q,Q_0} \quad (6)$$

Where M_Q is corrected chamber response, $D_{w,Q}$ is the water absorbed dose at the Q beam quality, k_{Q,Q_0} is the beam quality conversion factor, and N_{D,w,Q_0} shows the chamber calibration factor at reference beam quality of Q_0 . Then, the radiation absorbed dose at the depth of maximum dose (D_{max}) can be calculated through EQUATION (7). PDD (z_{ref}) is percentage depth dose at reference depth (z_{ref}) in field size of 10 cm x 10 cm.

$$D_{max} = M_Q N_{DwQ_0} k_{Q,Q_0} / PDD(z_{ref}) \quad (7)$$

M_Q is a corrected detector reading by the correction factor of k_{TP} , k_{pol} , k_s , and h_{pl} . The M_Q value is expressed in EQUATION (8). M_1 is chamber response at standard voltage, h_{pl} is the fluence scale factor as the characteristic of phantom slab material. The measurement correction factor values are used to correct the M detector reading to obtain the corrected detector reading value (M_Q).

$$M_Q = M_1 k_{TP} k_{pol} k_s h_{pl} \quad (8)$$

The calculation of the correction factors are as follows:

- k_{TP} means correction factor of temperature and cavity air pressure at reference conditions 20°C and 101.325 kPa [12,23]. The magnitude of this correction factor can be determined by EQUATION (9), while T and P are temperature and cavity air pressure, respectively.

$$k_{TP} = \frac{(273.2 + T)P_0}{(273.2 + T_0)P} \quad (9)$$

- k_{Q,Q_0} is correction factor of ionization chamber detector which calibrated with ^{60}Co at reference condition.
- k_{pol} is correction factor for ionization detector response to the effect of voltage polarity changing that given to the detector. The values of k_{pol} can be calculated with EQUATION (10) where M_- is the negative polarity electromagnet readings and M_+ is electrometer reading at positive polarity. While M means the electrometer reading gained at the routinely polarity used (negative or positive). The M_+ and M_- readings have to be ensured that the chamber reading is stable succeeding any polarity changes (several chambers need around 20 min to stabilize) [9,11,12].

$$k_{pol} = \frac{|M_+| + |M_-|}{2M} \quad (10)$$

- k_s is recombination correction factor which is the response of ionization detector due to an inadequate collection of charge in the ionization chamber cavity. Initial recombination value is normally less than 0.2% for radiation beams except heavy ions [12]. The value of k_s can be calculated using EQUATION (11), where α_0 , α_1 , and α_2 are constant, M_1 is the chamber's response in normal voltage and M_2 is the chamber's response in reduced voltage [9,11,12].

$$k_s = \alpha_0 + \alpha_1 \left(\frac{M_1}{M_2} \right) + \alpha_2 \left(\frac{M_1}{M_2} \right)^2 \quad (11)$$

Correction Factor of Slab Phantom to Water Phantom (CF)

The correction factor of slab phantom to water phantom can be calculated with EQUATION (12). Where D_{water} is absorbed dose rate of water phantom and D_{slab} is absorbed dose rate of slab phantom.

$$CF = \frac{D_{water}}{D_{slab}} \quad (12)$$

RESULT AND DISCUSSION

The measurement of LINAC output dose is part of the Quality Assurance (QA) program and the Quality Control (QC) of radiotherapy facilities [7]. Quality Assurance is a regular program or activity to ensure the consistency of medical stages [8]. Whereas QC is a routine measurement action carried out to monitor visual performance and equipment performance testing so that the output quality can be guaranteed. One series of QA and QC is the calibration or radiation dose measurement, including daily, weekly, monthly, and annual calibration. The measurement of PDD, beam quality value (TPR), and all correction factors to obtain the CF are shown below.

Percent Depth Dose (PDD)

FIGURE 3 shows the different charts of PDD photons and electrons. After reaching the maximum dose, the radiation dose of electrons tends to run out at a depth of 5-7 cm, while the radiation dose of the photon remains to a depth of 30 cm. This phenomenon is related to photon and electron radiation's penetrating power when interacting with the medium. From FIGURE 3 it can also be noted that the depth at the maximum dose rises as the increasing of electron beam energy.

Photon attenuation is greater than electron because photons have no mass. Therefore, in practice, the radiation photons used to treat inside cancer, while the electrons are used to treat

the surface cancer (usually located in skin surface). When the radiation of photon and electron interact with the phantom surface, the absorption dose on the surface is not 100% but will increase and reach the maximum 100% on some depth. Then the absorption dose will decrease according to the type and radiation energy. The probability of absorption dose to medium depends on the material density: the greater material density, the smaller absorption dose through the medium. Based on the PDD chart in FIGURE 3, the radiation quality values are obtained as in TABLE 1. The PDD parameters (R_{50}) would be raised with the electron beam energy increment, owing to the improved penetration ability of electron beam within the water at higher energies [13].

TABLE 1. The beam quality value

Radiation	Energy (MeV)	Beam Quality Value (Q)
Photon	6	$TPR_{20,10}=0.68$
Electron	6	$R_{50} = 2.42 \text{ g/cm}^2$
Electron	8	$R_{50} = 3.24 \text{ g/cm}^2$
Electron	10	$R_{50} = 4.02 \text{ g/cm}^2$
Electron	12	$R_{50} = 4.73 \text{ g/cm}^2$

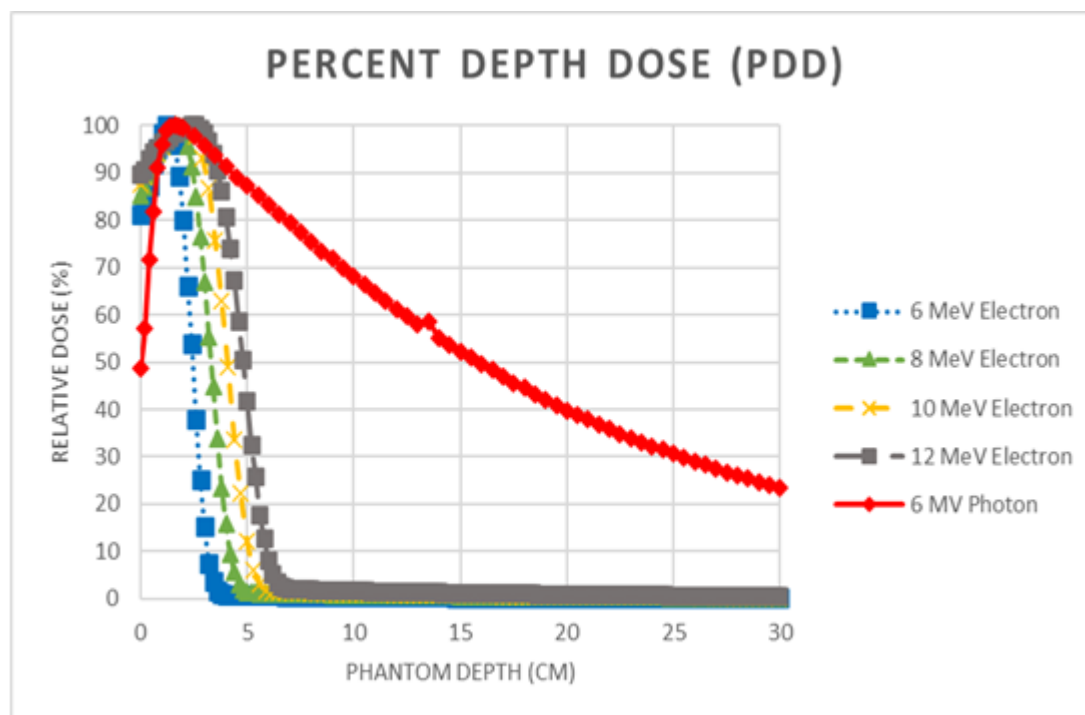


FIGURE 3: PDD profile as a depth function for photon and electron at various energy

Reference Depth

The reference depth (z_{ref}) can be calculated from the radiation quality value using EQUATIONS (3), (4) and (5), see TABLE 2. After getting the z_{ref} value, the absolute dosimetry measurement is conducted by placing the detector on z_{ref} . Samira Yazdani et al also investigated the reference depth (z_{ref}) for commissioning and validation of Varian LINAC and obtained z_{ref} for 6,10,12 MeV electron equal to 1.3, 2, and 2.8 cm, respectively, which were in congruence with our results [8].

Correction Factors measurement and corrected dosimetry reading value

From the data measurement, the correction factors can be obtained through EQUATIONS (9), (10), (11), that shown in TABLE 3 and TABLE 4.

The corrected dosimetry reading value (MQ) can be calculated using Equation (8) which shown in TABLE 5.

TABLE 2. Reference Depth (Z_{ref})

Radiation	Energy	Z_{ref} (cm)
Photon	6 MV	10
Electron	6 MeV	1.4
Electron	8 MeV	1.8
Electron	10 MeV	2.3
Electron	12 MeV	2.7

TABLE 3. Correction factors of Water Phantom

Correction Factors	Photon		Electron		
	6 MV	6 MeV	8MeV	10 MeV	12 MeV
k_{TP}	1.016	1.016	1.016	1.016	1.016
k_{pol}	1.001	1.001	1.002	1.001	1.001
k_s	1.002	1.006	1.006	1.007	1.007
$k_{Q,Q0}$	0.990	0.916	0.913	0.911	0.908
h_{pl}	1.002	1.002	1.002	1.002	1.002

TABLE 4. Correction factors of Slab Phantom

Correction Factors	Photon		Electron		
	6 MV	6 MeV	8MeV	10 MeV	12 MeV
k_{TP}	1.016	1.016	1.016	1.016	1.016
k_{pol}	1.001	1.003	1.003	1.001	1.001
k_s	1.001	1.006	1.006	1.007	1.007
$k_{Q,Q0}$	0.990	0.916	0.913	0.911	0.908
h_{pl}	1.019	1.019	1.019	1.019	1.019

TABLE 5. Correction dosimetry reading value (MQ)

Radiation	Energy	Z_{ref} (cm)	
		Water phantom	Slab phantom
Photon	6 MV	0.1257	0.1254
Electron	6 MeV	0.1996	0.1997
Electron	8 MeV	0.2037	0.2041
Electron	10 MeV	0.2043	0.2034
Electron	12 MeV	0.2048	0.2034

We also compared the correction factor value with another publication that was carried out by Baghani et.al [11] who characterized several cylindrical ion chamber dosimeters on high energy photons produced by a LINAC Varian Trilogy using TRS-398 protocol. Those correction factors data are obtained from the same type of cylindrical ionization chamber, TM 30013. The benchmarking results are shown in FIGURE 4 where the correction factor value of the current study shows a good agreement with the difference of correction factor value below 0.2%, while the difference value for $TPR_{20,10}$ is around 1.82%.

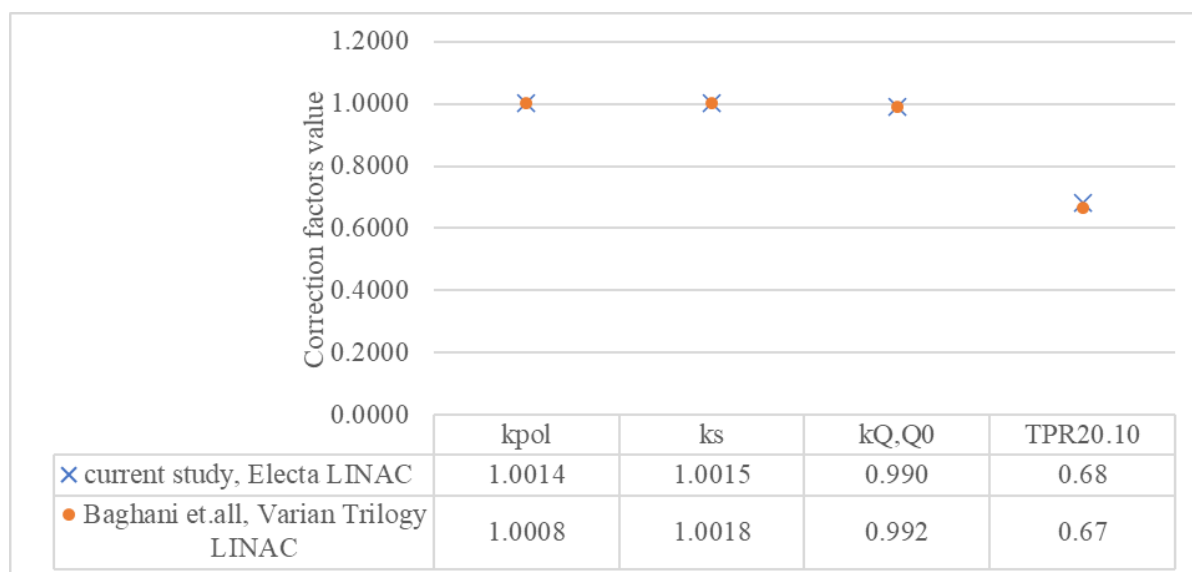


FIGURE 4: Benchmarking of correction factor value with previous work[11]

Absorbed dose

Having a role as the basic physical amount in radiology and radiological protection, absorbed dose is applied for all types of ionizing radiation and any irradiation geometry. Absorbed dose is the amount of dose measured in energy per unit mass of a material after exposure to ionizing radiation [24,25]. The absorbed dose expressed in gray (Gy) and the SI unit is J.kg^{-1} . The absorbed dose (see TABLE 6) is obtained from the mean value of the stochastic amount of energy emitted and therefore does not represent the random fluctuations of the interaction events in tissue. That is defined at any point in material and, in principle, is a measurable quantity. The absorbing dose rate was transformed into annual effective dose equivalent with a conversion factor value of 0.7 SvGy^{-1} suggested by the United Nations Scientific Committee of the effect of Atomic Radiation (UNSCEAR) [26]. The conversion factor of 0.2 is applied for outdoor occupancy by considering that most people spent their time outdoors for around 20% [27,28].

This absolute dosimetry measurement is carried out at 200 MU. The measurement of absorbed doses on phantom is one of the calibrations which sees the equality of LINAC output doses recorded in gantry in MU units with doses absorbed by a phantom in cGy units. Therefore, the final results obtained from absolute dosimetry measurements are made in units of cGy/MU.

TABLE 6 shows good agreement between measuring the absorbed dose by the water phantom and the slab phantom at the equivalent scale depth. The maximum dosimetry difference obtained is less than 1% for all electron and photon energies. These findings confirm the validity of using slab phantom in determining LINAC's calibration factors and absolute dosimetry. The results of this study are also reinforced by the findings of Hamid Reza Baghani and Mostafa Robotjazi [13]. They measured the scaling factor in the calibration of intraoperative electron beams using PMMA phantom plastic in Iran with relative difference less than 1%.

TABLE 6. The absorbed dose rate

Radiation	Energy	Absorbed dose rate (cGy/MU)		Relative difference (%)
		Water phantom	Slab phantom	
Photon	6 MV	0.9917	0.9898	-0.19%
Electron	6 MeV	0.9876	0.9881	0.05%
Electron	8 MeV	0.9972	0.9993	0.21%
Electron	10 MeV	0.9977	0.9937	-0.40%
Electron	12 MeV	0.9981	0.9913	-0.68%

Correction factors of slab phantom on water phantom

The slab phantom is used on LINAC calibration as a substitute phantom when the water phantom cannot be operated. In practice, water phantoms often get disturbances such as damage to detector mobilization tools, jammed water taps, and other more complex technical disturbances. This is because water phantom requires difficult maintenance and long preparation time. Therefore, many types of phantoms are made replacing water phantoms such as plastic water phantom, solid water phantom, virtual water phantom, PMMA, and polystyrene phantom. The slab phantom in this measurement is a type of white polystyrene phantom.

In many hospitals in Indonesia including in Dr. RSUP SARDJITO, the slab phantom was used as a phantom at LINAC's daily calibration. As a phantom for replacing water phantom (standard phantom), a slab phantom correction factor is needed for the water phantom in this daily calibration. The correction factor value (CF) is useful to find out the absorption dose in water phantom by absorbing doses on slab phantom multiplied by the correction factor. Based on Equation (12), the slab phantom correction factor for water phantom was obtained in this study which can be seen in TABLE 7.

Based on the correction factor values in TABLE 7, the slab phantom absorbed dose value in electron dosimetry of 6 MeV and 8 MeV is greater than the radiation absorbance dose in the water phantom. According to the theory, the absorbed dose of radiation in the slab phantom should be smaller than the radiation absorbed dose in the water phantom. The probability of radiation interacting with the slab phantom material is greater than the probability of radiation interacting with water phantom because the slab phantom density is higher than the water phantom. This causes the radiation dose absorbed before reaching the detector in the slab phantom is more than the water phantom so that the absorbed dose received by the detector on the slab phantom is smaller.

TABLE 7. The correction factor of slab phantom on water phantom

Radiation	Energy	Correction Factor (CF)
Photon	6 MV	1.0018
Electron	6 MeV	0.9995
Electron	8 MeV	0.9979
Electron	10 MeV	1.0041
Electron	12 MeV	1.0068

The factors that influence the deviation results in electron dosimetry of 6 MeV and 8 MeV are types of detectors. Each detector has different functions and specifications. The detector used in this measurement is an ionized cylindrical chamber detector. While ionization chambers of

cylindrical type can be utilized to calibrate electron beams at energies of more than 10 MeV, the TRS-398 dosimetry protocol states that it is recommended to use the parallel-plate ionization chamber type when calibrating the electron beam over all energy ranges [9,12].

The cylindrical ionization chamber detector is good for dosimetry of high energy photons and high energy electron dosimetry with an energy of higher than 10 MeV. In the dosimetry of electrons with energy <10 MeV, a plane-parallel ionization chamber detector is more sensitive than an ionized chamber cylindrical detector. The plane-parallel ionization chamber detector is able to minimize perturbation effect scattering on energy electrons <10 MeV because the active volume of small plane-parallel detectors is 0.02 cm^3 , while cylindrical ionization chambers have a larger active volume of 0.6 cm^3 . Scattering perturbation is the effect that arises due to interference from radiation scattering. The lower the radiation energy the greater the probability of scattered radiation. This causes the absorption dose of slab phantom to be greater than the water phantom in the 6 MeV and 8 MeV energy electrons in the measurement using an ionized cylindrical chamber detector.

This result of the slab phantom correction factor for the water phantom was made as a correction when the slab phantom was used for LINAC daily calibration. The slab phantom correction factor value of the water phantom in the absolute dosimetry of the 6 MV photon beam, 6 MeV electron, 8 MeV electron, 10 MeV electron and 12 MeV electron respectively are 1.0018; 0.9995; 0.9979; 1.0041 and 1.0068. Using this correction factor, the calibration of photon and electron beam can be carried out on the slab phantom material.

CONCLUSION

Determination of the correction factor value of slab phantom for water phantom is a key element in quality management system of dose accuracy received by the patient. Therefore, the calibration of LINAC will be more accuracy and efficient. The slab phantom's correction factor value based on the water phantom in absolute dosimetry of photon beam 6 MV, 6 MeV electron, 8 MeV electron, 10 MeV electron and 12 MeV electron LINAC Elekta Synergy Platform 154029 plane are 1.0018; 0.9995; 0.9979; 1.0041, and 1.0068. Benchmarking results of correction factor values include correction factor of polarity (k_{pol}), a correction factor of recombination (k_s), and conversion factor for beam quality ($k_{Q,Q0}$) with other published reference data showing that the correction factor value for absolute dosimetry calculations has a good agreement. Therefore, it can be used for Elekta and Varian LINAC calibrations.

ACKNOWLEDGEMENT

The author would like to thank the Nuclear Engineering and Engineering Physics Department of Universitas Gadjah Mada and the Radiotherapy Installation of Dr. RSUP SARDJITO for the support, assistance, and advice for the completion of this research.

REFERENCES

- [1] R. Baskar *et al.*, "Biological response of cancer cells to radiation treatment," *Frontiers in molecular biosciences*, vol. 1, p. 24, 2014.

- [2] N. Ade, D. Van Eeden and F. C. P. du Plessis, "Characterization of Nylon-12 as a water-equivalent solid phantom material for dosimetric measurements in therapeutic photon and electron beams," *Applied Radiation and Isotopes*, vol. 155, p. 108919, 2020.
- [3] B. Tiwari *et al.*, "Tissue-equivalent dosimeters based on copper doped lithium tetraborate single crystals for radiotherapy," *Radiation Measurements*, vol. 151, p. 106704, 2022.
- [4] D. A. Jaffray and M. K. Gospodarowicz, "Radiation Therapy for Cancer," In: Gelband H, Jha P, Sankaranarayanan R, Horton S, editors, Washington (DC), 2015.
- [5] A. Lima-Flores *et al.*, "Analysis and characterization of neutron scattering of a Linear Accelerator (LINAC) on medical applications," *Journal of Nuclear Physics, Material Sciences, Radiation and Applications*, vol. 5, no 1, pp. 65-78, 2017.
- [6] I. Rosenberg, "Radiation Oncology Physics: A Handbook for Teachers and Students," *British Journal of Cancer*, vol. 98, no. 5, p. 1020, 2008.
- [7] M. Bencheikh, A. Maghnouj and J. Tajmouati, "Dosimetry quality control based on percent depth dose rate variation for checking beam quality in radiotherapy," *Reports of Practical Oncology and Radiotherapy*, vol. 25, no. 4, pp. 484-488, 2020.
- [8] S. Yazdani, F. S. Takabi and A. Nickfarjam, "The commissioning and validation of eclipseTM treatment planning system on a varian vitalbeamTM medical linear accelerator for photon and electron beams," *Frontiers in Biomedical Technologies*, vol. 8, no. 2, pp. 102-114, 2021.
- [9] H. R. Baghani, M. Robotjazi and S. Andreoli, "Comparing the dosimeter-specific corrections for influence quantities of some parallel-plate ionization chambers in conventional electron beam dosimetry," *Applied Radiation and Isotopes*, vol. 179, p. 110031, 2022.
- [10] J. Renaud *et al.*, "Absorbed dose calorimetry," *Physics in medicine and biology*, vol. 65, no. 5, p. 05TR02, 2020.
- [11] H. R. Baghani, S. Andreoli and M. Robotjazi, "Performance characteristics of some cylindrical ion chamber dosimeters in Megavoltage (MV) photon beam according to TRS-398 dosimetry protocol," *Radiation Physics and Chemistry*, vol. 180, pp. 109299, 2021.
- [12] P. Andreo *et al.*, "IAEA Technical Report Series No.398," *Absorbed Dose Determination in External Beam Radiotherapy*, International Atomic Energy Agency, Vienna, vol. 398, 2006.
- [13] H. R. Baghani and M. Robotjazi, "Scaling factors measurement for intraoperative electron beam calibration inside PMMA plastic phantom," *Measurement: Journal of the International Measurement Confederation*, vol. 165, p. 108096, 2020.
- [14] G. Martin-Martin *et al.*, "Assessment of ion recombination correction and polarity effects for specific ionization chambers in flattening-filter-free photon beams," *Physica Medica*, vol. 67, pp. 176-84, 2019.
- [15] S. A. Pawiro *et al.*, "Modified electron beam output calibration based on IAEA Technical Report Series 398," *Journal of applied clinical medical physics*, vol. 23, no. 4, p. e13573, 2022.

- [16] M. Pimpinella, L. Silvi and M. Pinto, "Calculation of k Q factors for Farmer-type ionization chambers following the recent recommendations on new key dosimetry data," *Physica Medica*, vol. 57, pp. 221-230, 2019.
- [17] J. Madamesila *et al.*, "Characterizing 3D printing in the fabrication of variable density phantoms for quality assurance of radiotherapy," *Physica Medica*, vol. 32, no. 1, pp. 242-247, 2016.
- [18] A. Pehlivanlı and M. H. Bölükdemir, "Investigation of the effects of biomaterials on proton Bragg peak and secondary neutron production by the Monte Carlo method in the slab head phantom," *Applied Radiation and Isotopes*, vol. 180, pp. 1-7, 2022.
- [19] M. Bencheikh, A. Maghnoij and J. Tajmouati, "Mathematical parameterization of dosimetry quality index checking of the photon beam based on IAEA TRS-398 protocol," *Journal of King Saud University - Science*, vol. 31, no. 4, pp. 1543-1546, 2019.
- [20] A. Fauzi, Darmawati and F. Aliyah, "Penentuan Faktor Koreksi Slab Phantom Terhadap Water Phantom Pada Dosimetri Absolut Berkas Foton Dan Elektron Pesawat Linac Berdasarkan Iaea Trs-398," Universitas Gadjah Mada, 2018.
- [21] D. K. Bewley, "Central axis depth dose data for use in radiotherapy, A survey of depth doses and related data measured in water or equivalent media," *British journal of radiology Supplement*, vol. 17, pp. 1-147, 1983.
- [22] E. B. Podgorsak, "Radiation Oncology Physics: A Handbook for Teachers and Students," IAEA. Vienna: IAEA, pp. 249-292, 2005.
- [23] S. Vynckier, Heijmen *et al.*, "Code of Practice for the Absorbed Dose Determination in High Energy Photon and Electron Beams," Netherland, 2012.
- [24] N. Ipe, "Shielding Design and Radiation Safety of Charged Particle Therapy Facilities, PTCOG Report 1," *Particle Therapy Cooperative Group (PTCOG)*, 2010.
- [25] E. Vano *et al.*, "Dosimetric quantities and effective dose in medical imaging: a summary for medical doctors," *Insights into Imaging*, vol. 12, no. 1, p. 99, 2021.
- [26] S. Unscear, "effects of Ionizing Radiation," United Nations, New York, pp. 453-487, 2000.
- [27] K. Debertin and R. G. Helmer, "Gamma- and X-ray spectrometry with semiconductor detectors," Netherlands: North-Holland, 1988.
- [28] A. Miah *et al.*, "Natural Radioactivity and Associated Dose Rates in Soil Samples of Malnichera Tea Garden in Sylhet District of Bangladesh," *Journal of Nuclear and Particle Physics*, vol. 2, no. 6, pp. 147-152, 2013.